Supplement of Atmos. Meas. Tech., 9, 3687–3706, 2016
http://www.atmos-meas-tech.net/9/3687/2016/
doi:10.5194/amt-9-3687-2016-supplement


Atmospheric Measurement Techniques
Open Access
EGU

*Supplement of*

# A new set-up for simultaneous high-precision measurements of $CO_2$, $\delta^{13}$C-$CO_2$ and $\delta^{18}$O-$CO_2$ on small ice core samples

**Theo Manuel Jenk et al.**

*Correspondence to:* Theo Manuel Jenk (theo.jenk@psi.ch)

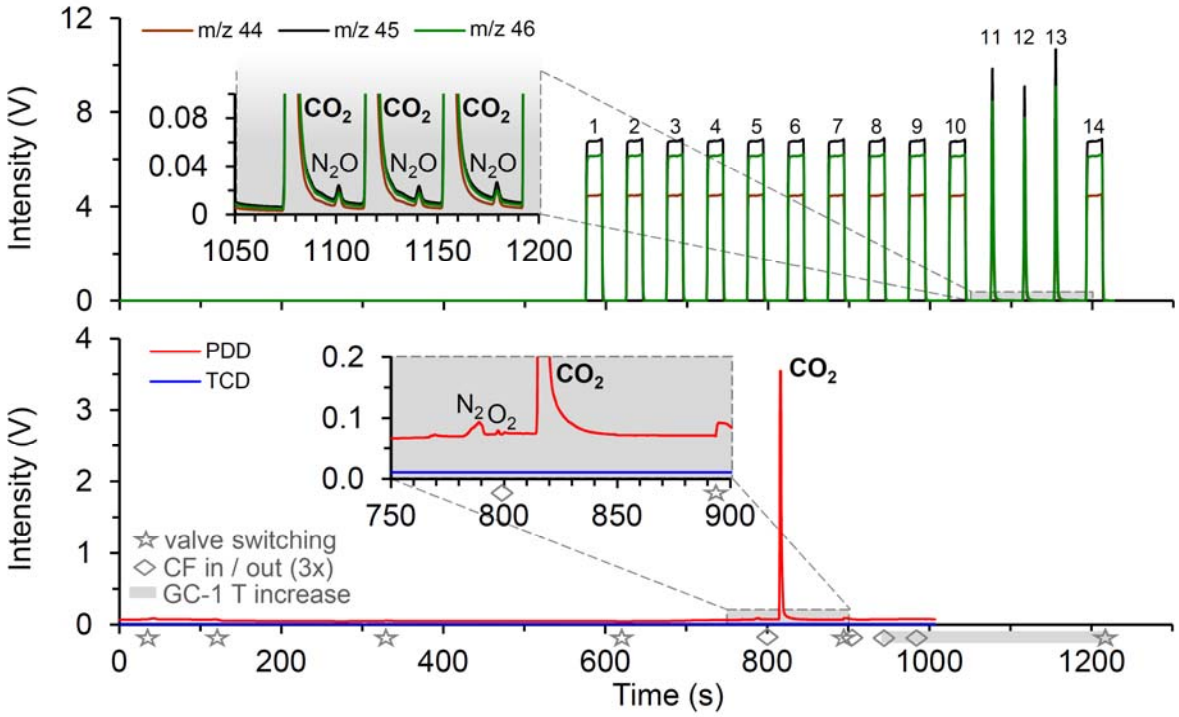


**Figure S1:** Chromatograms for the measurement of pure $CO_2$-WS injected into section B of the setup (Fig. 2 in the main manuscript) and subsequently passing the PreCon–GC system. Upper panel: IRMS signal intensity for mass 44, 45, and 46. Injections of the WS via the open split are identifiable by the flat-topped peaks. Peaks 1-9 are used to reach stable source conditions while peaks 10 and 14 before and after the samples (i.e. the WS passing the PreCon–GC system) are used for referencing. The inset shows baseline details and $N_2O$ separation in detail. Lower panel: PDD and TCD intensity signal for $CO_2$ and air (not detected for the pure $CO_2$ sample injected here), respectively. Stars indicate valve switching, resulting in small variations in the PDD signal due to changes in pressure and flow (see inset, not detected by the less sensitive TCD). Diamonds indicate immersion of the three capillary traps into liquid nitrogen for $CO_2$ cryofocusing and their subsequent one by one release resulting in the three peaks of the split sample shown in the upper panel (peaks 11–13). Over the time period indicated by the grey bar the GC–1 temperature is increased to 150 °C in order to precondition the column for the next sample. The enlargement shows baseline details and the $N_2$ and $O_2$ signal of the system blank contribution.

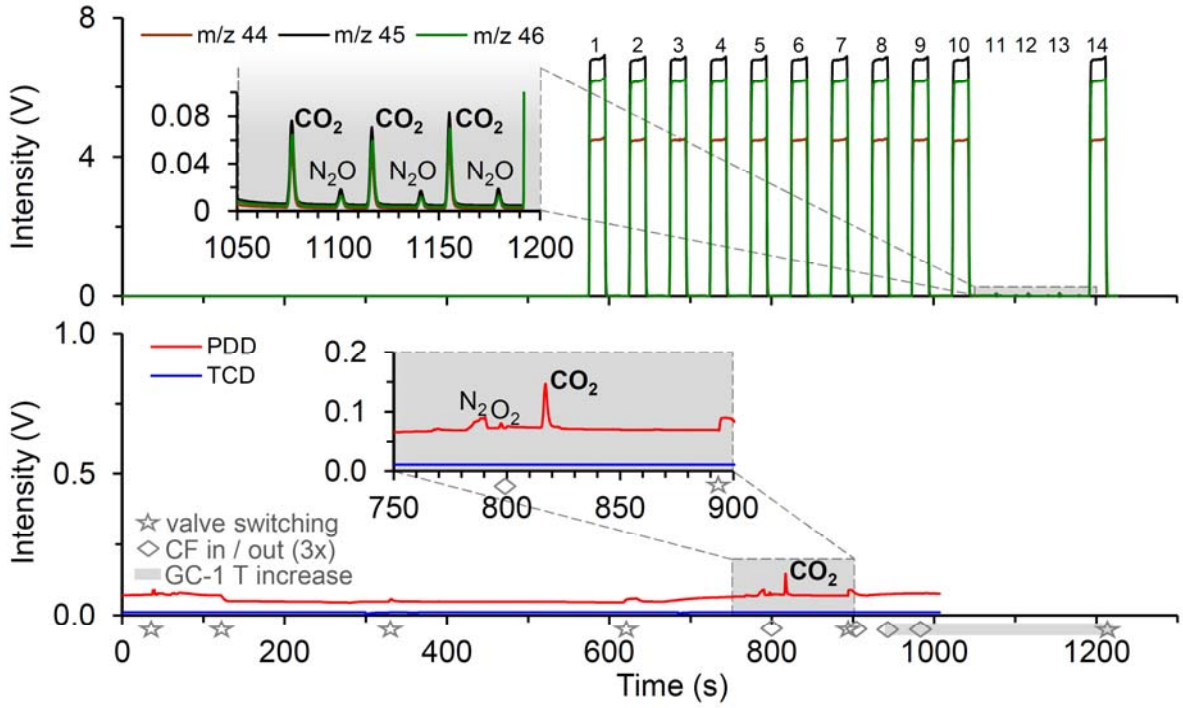


**Figure S2:** Chromatograms for the measurement of a system blank including both sections A and B (Fig. 2) and bellow compression (i.e. needle movement without ice). Upper panel: IRMS signal intensity for mass 44, 45, and 46. Injections of the WS via the open split are identifiable by the flat-topped peaks. Peaks 1–9 are used to reach stable source conditions while peaks 10 and 14 before and after the samples (i.e. the system blank) are used for referencing. The inset shows baseline details and the system blank signal of $CO_2$ and $N_2O$ in detail. Lower panel: PDD and TCD intensity signal for $CO_2$ and air (not detected), respectively. Stars indicate valve switching, resulting in small variations in the PDD signal due to changes in pressure and flow (see inset, not detected by the less sensitive TCD). Diamonds indicate immersion of the three capillary traps into liquid nitrogen for $CO_2$ cryofocusing and their subsequent one by one release resulting in the three peaks of the split sample shown in the upper panel (peaks 11–13). Over the time period indicated by the grey bar the GC–1 temperature is increased to 150 °C in order to precondition the column for the next sample. The enlargement shows baseline details and the system blank contribution of $N_2$, $O_2$ and $CO_2$.

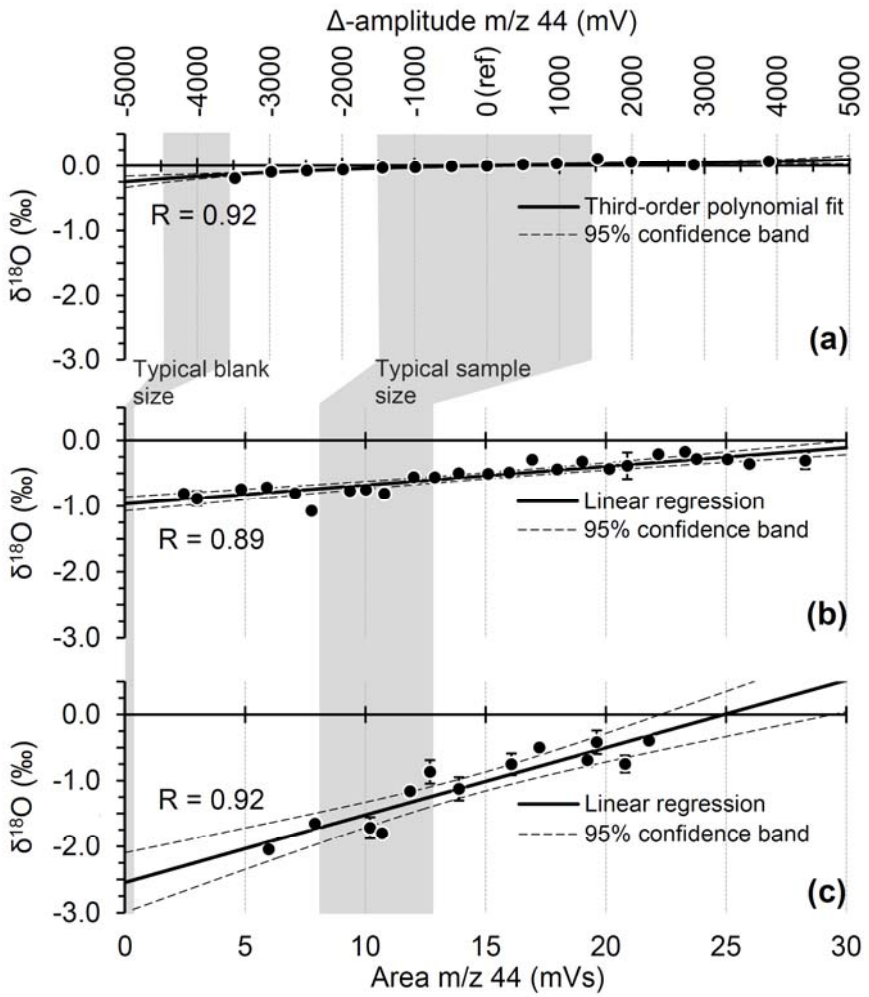


**Figure S3:** Fractionation effects for $\delta^{18}O$: (a) IRMS nonlinearity effect; $\delta^{18}O$ dependence on peak amplitude (top *x* axis), Δ–amplitude is the deviation in intensity (m/z 44) from the reference peak (ref, $\delta^{18}O$ and Δ–amplitude = 0). The data are obtained from a total of 177 measurements and mean values with the 1$\sigma$ standard deviation are shown. (b) PreCon–GC linearity (bottom *x* axis); $CO_2$ sample size dependence for pure $CO_2$ working standard directly injected to section B. The data are obtained from a total of 318 measurements corrected for IRMS nonlinearity and blank; mean values with the 1$\sigma$ standard deviation are shown. (c) Air amount dependence (bottom *x* axis); air sample size dependence for air standards/samples injected to section A. The data are obtained from a total of 46 measurements corrected for IRMS nonlinearity, PreCon–GC linearity and system blank. Mean values with the 1$\sigma$ standard deviation are shown. The grey bars indicate the typical procedural blank and sample size range of air extracted from ice samples, respectively.

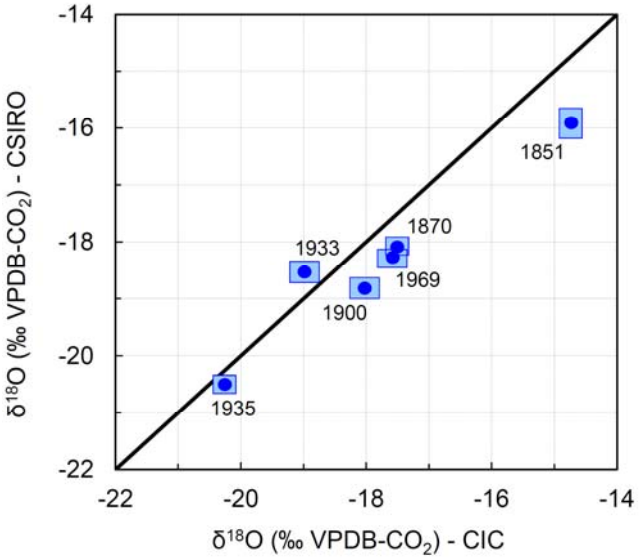


**Figure S4:** Laboratory comparison measurements of Law Dome ice samples covering the recent past (1851–1969 AD). $\delta^{18}O\text{-}CO_2$ values measured at CIC (*x* axis) and CSIRO (*y* axis; M. Rubino, pers. comm.) are shown. Blue boxes indicate 1$\sigma$ uncertainties defined for each laboratory by the respective side length.

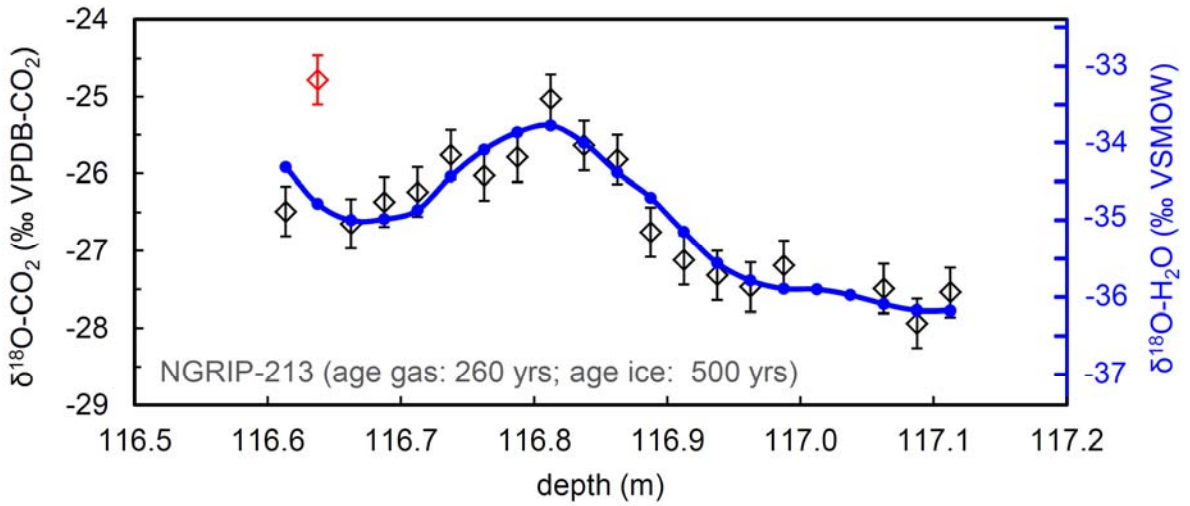


**Figure S5:** High resolution records of $\delta^{18}O\text{-}CO_2$ with error bars ($1\sigma$, left axis) and $\delta^{18}O\text{-}H_2O$ (right axis) for an ice section from NGRIP. The sample in red has been defined as an outlier (for details see Sect. 4.3 in the main manuscript).